

Exact time-dependent density functional theory for impurity models

P. Schmitteckert^{1,2}, M. Dzierzawa³ and P. Schwab³

¹ *Institute of Nanotechnology, Karlsruhe Institute of Technology, 76021 Eggenstein-Leopoldshafen, Germany*

² *Center of Functional Nanostructures, Karlsruhe Institute of Technology, 76131 Karlsruhe, Germany and*

³ *Institut für Physik, Universität Augsburg, 86135 Augsburg, Germany*

(Dated: March 4, 2013)

We employ the density matrix renormalization group to construct the exact time-dependent exchange correlation potential for an impurity model with an applied transport voltage. Even for short-ranged interaction we find an infinitely long-ranged exchange correlation potential which is built up instantly after switching on the voltage. Our result demonstrates the fundamental difficulties of transport calculations based on time-dependent density functional theory. While formally the approach works, important information can be missing in the ground-state functionals and may be hidden in the usually unknown non-equilibrium functionals.

I. INTRODUCTION

In recent years a combination of Kohn-Sham density functional theory (DFT) and the Landauer approach to transport has been developed that allows an ab-initio calculation of the current-voltage characteristics of molecules that are attached to reservoirs. Early comparisons between calculated and experimental conductances yielded discrepancies of several orders of magnitude, while in more recent comparisons a typical discrepancy of one order of magnitude was reported.¹ Concerning experiments, the reproducibility of I - V characteristics in molecular electronics poses a problem, as the contact configuration may change from sample to sample, which makes the comparison between theory and experiment difficult.

First DFT studies of lattice models like the Hubbard model or spinless fermions date already back to the late 1980s.^{3–5} At that time ground state DFT was the main focus of interest. In the 2000s a lattice version of the local density approximation was constructed using the Bethe ansatz solution of the Hubbard model, and the accuracy of the method was tested in some detail.^{6–8} Due to the mentioned discrepancies between measured and calculated conductances through molecules, recently the focus turned to the DFT description of transport. In the conventional DFT approach to the two-terminal linear conductance of a molecular system the Kohn-Sham equations are solved in order to obtain the electronic structure, and the conductance of the Kohn-Sham system, G_{KS} , is used as a theoretical estimate of the true conductance, G . There are thus two possible sources for errors, (i) the electronic structure calculation and (ii) the identification of G with G_{KS} . While in complex realistic structures it is not possible to quantify (i) and (ii) this is possible for lattice models, as demonstrated by Schmitteckert and Evers.⁹ They observed that the Kohn-Sham conductance, G_{KS} , based on the exact ground state exchange correlation potentials becomes accurate, i.e. $G_{\text{KS}} = G$, close to (isolated) conductance resonances. Remarkably this holds even if the spectral properties of the Kohn-Sham system strongly differ from the true ones.^{9,10} For example, the zero temperature conductance through a

Kondo impurity is captured correctly by G_{KS} . The reason for this coincidence is the Friedel sum rule which guarantees that G and G_{KS} have identical functional dependencies on the charge density.^{9,11,12} However, as soon as the conductance is not given by a local Friedel sum rule there can be orders of magnitude between G_{KS} and the true conductance,^{10,13,14} and it can even be parametrically wrong.¹⁵ It is important to note that this is not a general failure of DFT; rather the assumption that the conductance of the physical electrons is given by the conductance of the Kohn-Sham particles breaks down. It has been stated several times in the literature that this discrepancy can be corrected by including dynamic contributions to the exchange-correlation potential that are not captured by ground state functionals.^{16–18} For the linear current I through an impurity this dynamic exchange-correlation potential V^{xc} renormalizes the voltage, such that

$$I = GV = G_{\text{KS}}(V + V^{\text{xc}}). \quad (1)$$

It is not clear whether a similar voltage renormalization is also present in the non-linear response.

The goal of our study is to investigate the nature of the dynamical response within a DFT framework beyond the linear transport regime. To this end we construct the exact time-dependent exchange-correlation potential for an impurity model with an applied transport voltage. Specifically we construct the time-dependent Kohn-Sham potentials for a two-terminal transport setup, which by construction yields the correct physical current within the time-dependent DFT description. In this paper we will concentrate on a one-dimensional lattice model, where we can directly compare time-dependent DFT with accurate numerical and analytical results obtained by many-body techniques.² In order to obtain meaningful results we have to solve much larger systems (here: 240 lattice sites) than for instance in Ref. 19 (6 to 12 lattice sites). In addition the densities have to be calculated with an accuracy better than $\sim 10^{-6}$; otherwise the reverse engineering of the time-dependent exchange-correlation potentials fails.

We consider the interacting resonant level model, i.e. a one-dimensional model of spinless fermions, where a

single interacting level is coupled to a left and a right lead,

$$H = H_L + H_{LR} + H_R \quad (2)$$

$$H_L = -t \sum_{i=1}^{N_L-1} c_{Li}^\dagger c_{Li+1} + \text{h.c.} \quad (3)$$

$$H_R = -t \sum_{i=1}^{N_R-1} c_{Ri}^\dagger c_{Ri+1} + \text{h.c.} \quad (4)$$

$$H_{LR} = -t'(c^\dagger c_{L,1} + c^\dagger c_{R,1} + \text{h.c.}) + U(n - 1/2)(n_{L,1} + n_{R,1} - 1). \quad (5)$$

Here $t = 1$ is the hopping amplitude, N_L and N_R are the numbers of sites in the left and right lead, and U is the interaction on the contact link. All the data presented in this article have been obtained for the half-filled lattice model. We assume that at time $T < 0$ the system is in the ground state. At $T = 0$ we include a voltage drop by applying a potential $eV/2$ ($-eV/2$) on the left (right) lead with a linear crossover on a scale of several sites left and right of the impurity. Then we follow the time evolution of the system. On time scales that are shorter than the transit time $T_t = L_{\text{lead}}/v_F$ ($v_F = 2t$ is the Fermi velocity) the finite leads act as reservoirs, such that a time-dependent simulation allows to extract the current-voltage relation corresponding to infinite leads, see Refs. 2 and 20 for details. Note that in our model the linear conductance is given by a Friedel sum rule.^{9,21} Therefore, V^{xc} vanishes in the linear regime.

We consider a Hamiltonian H with parameters U and t' and a Kohn-Sham Hamiltonian H_{KS} with the same structure as Eq. (2) using different parameters $U_{\text{KS}} = 0$ and t'_{KS} . The essence of DFT is a one-to-one correspondence between local densities and potentials: Starting with an uniquely defined initial state there exists an – up to a gauge transformation – unique set of potentials $\{v_{\text{KS}}(T)\}$ such that the time-dependent densities $\{n(T)\}$ are identical for H and H_{KS} . The numerical task is to calculate first the time-dependent local density for H and in the second step the set of potentials $\{v_{\text{KS}}\}$ for H_{KS} . We fix the gauge by imposing that the sum of the potentials is zero. To calculate the particle density we follow two strategies: (a) The particle density in an interacting system is obtained through time-dependent density matrix renormalization group (td-DMRG) as described in Refs. 20 and 22. Since these calculations are extremely time-consuming we also (b) study a toy model of non-interacting fermions, where the time-dependent density can be obtained straightforwardly by exact diagonalization. As mentioned before, when calculating $\{v_{\text{KS}}\}$ from the densities a high accuracy is necessary. We use an iterative procedure that stops when the densities in H and in H_{KS} agree within an error of 10^{-10} .

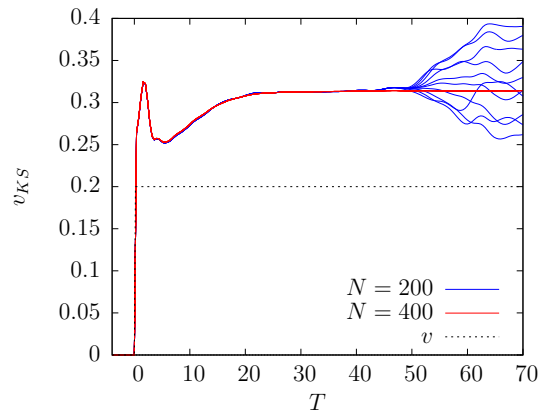


FIG. 1: The Kohn-Sham potential v_{KS} as a function of time for the first ten lattice sites from the left edge of the chain. The two data sets are for a total chain length $N = 200$ and $N = 400$. For comparison the potential $v = 0.2t$ in the toy model (corresponding to a voltage $eV = 0.4t$) is also shown as dotted line.

II. NONINTERACTING TOY MODEL

We start by considering the non-interacting version of the Hamiltonian (2), i.e. we set the interaction U as well as U_{KS} to zero. There remains only one free parameter, the hopping amplitude t' between the impurity site and the leads. In our toy model we choose $t' = 0.5t$ and $t'_{\text{KS}} = 0.3t$. Typical results for the time-dependent Kohn-Sham potentials are shown in Fig. 1. In the toy model a potential $eV = 0.4t$ corresponding to a potential $v = \pm 0.2t$ in the left (right) lead is switched on at $T = 0$. As a response a current flows through the resonant level that becomes stationary after $T \approx 30$ (the time is in units \hbar/t). By definition, the same current has to flow also in the Kohn-Sham system; here we find initially a time-dependent voltage which becomes stationary after $T \approx 30$. Remarkably the exchange-correlation potential (the difference between v_{KS} and v) is nearly position independent in the leads, and appears immediately after switching on the voltage. In the figure, data for a chain of 200 lattice sites and a chain of 400 lattice sites are presented. In both cases we plot the potentials for the first ten sites at the left edge of the chain. For the longer chain v_{KS} remains stationary until the end of the simulation, and only a single line is seen meaning that the potential is homogeneous in space. In the shorter chain the potential becomes position and time-dependent after $T \approx 50$. This happens since the simulation time is longer than the transit time $T_t = 100/2 = 50$.

The Kohn-Sham potential as a function of position is illustrated in Fig. 2, demonstrating that a major effect of the exchange-correlation potential is a time-independent renormalization of the local potentials, which implies an additional voltage as anticipated in Eq. (1). A reasonable estimate for the voltage renormalization is obtained by comparing the I - V characteristics for two noninter-

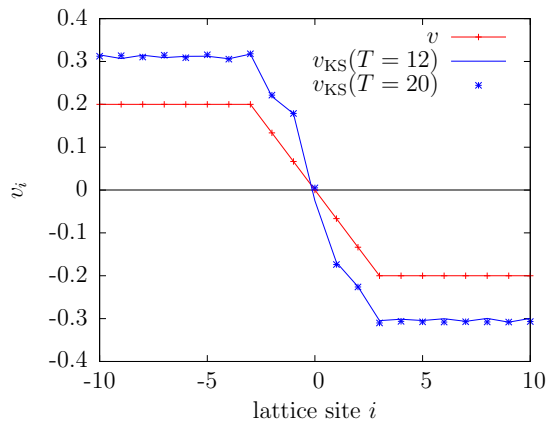


FIG. 2: Local potential v_i in the toy model and in the Kohn-Sham system close to the impurity ($i = 0$) at time $T = 12$ (solid curve) and $T = 20$ (symbols).

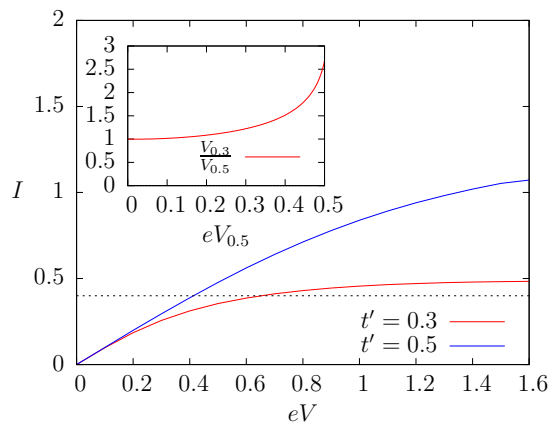


FIG. 3: Current (in units of et/h) as a function of voltage for two non-interacting systems with $t' = 0.3t$ and $t' = 0.5t$, respectively. In order to generate the same current in both systems (e.g. $I = 0.4$ as indicated by the dotted line) different potentials, $eV_{0.3}$ and $eV_{0.5}$, have to be applied. The voltage renormalization $V_{0.3}/V_{0.5}$ displayed in the inset gives a reasonable estimate of the voltage renormalization observed in the Kohn-Sham Hamiltonian for the toy model.

acting models with $t' = 0.3t$ and $t' = 0.5t$, see Fig. 3. The current $I = 0.3883$ (in units of et/h) corresponds to $eV = 0.4t$ for $t' = 0.5t$ and $eV = 0.6061t$ for $t' = 0.3t$ which is close to the voltage we found in the Kohn-Sham system, see Fig. 1. Notice that the maximum current that can be achieved is larger in the case $t' = 0.5t$ than for $t' = 0.3t$. For DFT this implies that no stationary Kohn-Sham potential can generate such large currents. Theoretically, time-dependent Kohn-Sham potentials could generate a stationary current, however, the proofs of existence of time-dependent Kohn-Sham potentials^{23–25} do not apply to the present situation, so that possibly the high voltages are not v -representable, compare Refs. 26 and 27. A similar situation will also arise in the next section where we investigate the model with interaction.

III. DMRG RESULTS FOR THE INTERACTING MODEL

We now turn our attention to the interacting case and choose H with $U = 2t$ and $t' = 0.3t$, whereas for the Kohn-Sham Hamiltonian we set $U_{\text{KS}} = 0$ and $t'_{\text{KS}} = 0.3t$. The I - V characteristics of this model is known analytically² from field theoretical methods. For example, the current is given in closed form by²⁹

$$I(V) = \frac{e^2 V}{2\pi\hbar} {}_3F_2 \left[\left\{ \frac{1}{4}, \frac{3}{4}, 1 \right\}, \left\{ \frac{5}{6}, \frac{7}{6} \right\}, -\left(\frac{V}{V_c} \right)^6 \right], \quad (6)$$

where ${}_3F_2$ is a hypergeometric function and $eV_c = rt^{4/3}$ sets the scale separating a charge $2e$ dominated low voltage regime, and a charge $e/2$ dominated high voltage regime.²⁸ The regularization $r \approx 3.2$ was determined from numerical simulation.^{2,28,29} The study of the toy model in the previous section shows that in order to obtain meaningful results the simulation time should be of the order $T \approx 30$ or longer, so that the length of each lead should be at least $L_{\text{lead}} \approx 60$ sites. This means that the excitations originating from the charge quench at the impurity should not reach the boundary of the leads within the simulation time. In order to obtain the time-dependent densities we apply the full td-DMRG²² as it has already proven to provide accurate results that agree perfectly with the analytic solution.

The quench with a symmetric charge imbalance leads to oscillations with frequency $eV/2$ during the transient time and finite size induced Josephson like oscillations with frequency eV in the steady state regime.²⁰ Therefore, when the effective voltage of the Kohn-Sham system is different from the voltage of the physical one, the time-dependent potentials have to compensate this mismatch. In order to reduce these finite time and finite size effects we ramp up the voltage linearly from $T = 0 \dots 5$, leading to reduced amplitudes of the transient oscillations. Fig. 4 shows the Kohn-Sham potential in the left lead. As in the non-interacting toy model the main effect is a voltage renormalization.

To obtain numerically converged data is a hard task. The figure shows results from three different DMRG runs varying the numerical accuracy. In all three runs the time-dependent particle density is almost identical, variations occur on the scale 10^{-6} . The Kohn-Sham potentials turn out to be very sensitive functions of the particle density and show pronounced differences in the three cases. Only for a very large number of states per block in the DMRG calculations (highest accuracy) the final result becomes smooth. In Fig. 5 time-dependent Kohn-Sham potentials for different voltages are depicted. Whereas for a small voltage we are able to find Kohn-Sham potentials for all times, this is not the case for large voltage where the Kohn-Sham potential diverges at finite T . It will be interesting to see in future research, whether the time scale of the singularity has a deeper meaning. Since the v -representability is not guaranteed in the lattice model,

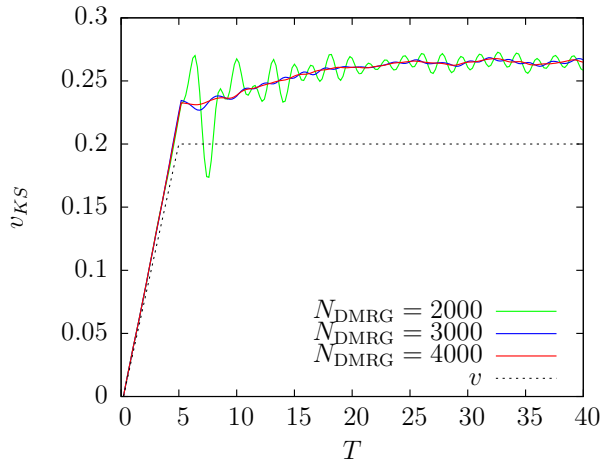


FIG. 4: Local potentials on the first ten sites of the left lead as a function of time for an interacting system ($U = 2t$, 240 lattice sites). Here we smoothly switched on the external voltage $V = 0.4t$ between $T = 0$ and $T = 5$. The number of states per block kept in the DMRG calculations varied between 2000 and 4000.

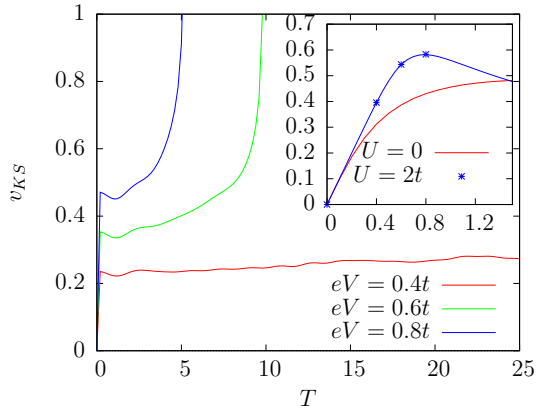


FIG. 5: Time-dependent Kohn-Sham potentials on the first ten sites of the left lead varying the voltage applied to the system ($t' = 0.3t$ and $U = 2t$). While for a small voltage ($eV = 0.4t$) we are able to find a set of Kohn-Sham potentials for all times, for larger voltages ($eV = 0.6t$, $eV = 0.8t$) this is only possible for short times. The inset shows the I - V characteristics for $U = 0$ and $U = 2t$. The curve for $U = 2t$ is given by Eq. (6) and the symbols are the DMRG results.

we believe that Kohn-Sham potentials do not exist for all times in these cases, compare also the discussion relating to Fig. 3.

In the inset of Fig. 5 we show the I - V characteristics of the noninteracting ($U = 0$) and interacting ($U = 2t$) resonant level model. Again, there is a regime, where the current in the interacting case is higher than any current achievable in the noninteracting case. Since the noninteracting case is similar to the Kohn-Sham system, this is a hint that no stationary Kohn-Sham potential might exist in this regime. The cases where we find diverging Kohn-Sham potentials are indeed in the regime where the current for $U = 2t$ exceeds the one for $U = 0$. Of course, the Kohn-Sham systems at finite voltage have additional potentials with a spatial structure which is not captured by a single number, V^{xc} . It is also important to note, that the Kohn-Sham potentials should not create a current outside the “light cone” $v_F T$. The continuity equation then implies that any oscillations of the potentials outside this regime have to be instantaneous and constant in space including the reservoirs. While one can gauge the resulting V^{xc} into a time-dependent phase $\exp(iV^{\text{xc}}T)$ of a hopping element at the impurity, one loses the property of an at least locally stationary system found in this work.

IV. SUMMARY

We calculated the exchange-correlation potential for a one-dimensional model system with an applied transport voltage. Specifically we considered an impurity model with short-ranged interaction and non-interacting leads. Immediately after switching on the voltage the exchange-correlation potential appears deep inside the leads. This long-ranged potential is purely dynamic, and therefore approximations based on equilibrium functionals and short-ranged approximations have to fail.

This work has been supported by the Deutsche Forschungsgemeinschaft through TRR80. We would like to thank Ferdinand Evers, Claudio Verdozzi, and Peter Wölfle for insightful discussions.

- ¹ S. M. Lindsay and M. A. Ratner, Adv. Mater. **19**, 23 (2007).
- ² E. Boulat, H. Saleur, and P. Schmitteckert, Phys. Rev. Lett. **101**, 140601 (2008).
- ³ O. Gunnarsson and K. Schönhammer, Phys. Rev. Lett. **56**, 1968 (1986).
- ⁴ K. Schönhammer and O. Gunnarsson, J. Phys. C **20**, 3675 (1987).
- ⁵ K. Schönhammer, O. Gunnarsson, and R. M. Noack, Phys. Rev. B **52**, 2504 (1995).
- ⁶ N. A. Lima, M. F. Silva, L. N. Oliveira, and K. Capelle,

- Phys. Rev. Lett. **90**, 146402 (2003).
- ⁷ S. Schenk, M. Dzierzawa, P. Schwab, and U. Eckern, Phys. Rev. B **78**, 165102 (2008).
- ⁸ M. Dzierzawa, U. Eckern, S. Schenk, and P. Schwab, Phys. Status Solidi B **246**, 941 (2009).
- ⁹ P. Schmitteckert and F. Evers, Phys. Rev. Lett. **100**, 086401 (2008).
- ¹⁰ P. Tröster, P. Schmitteckert, and F. Evers, Phys. Rev. B **85**, 115409 (2012).
- ¹¹ H. Mera, K. Kaasbjerg, Y. M. Niquet, and G. Stefanucci, Phys. Rev. B **81**, 035110 (2010).

- ¹² H. Mera and Y. M. Niquet, Phys. Rev. Lett. **105**, 216408 (2010).
- ¹³ J. P. Bergfield, Z.-F. Liu, K. Burke, and C. A. Stafford, Phys. Rev. Lett. **108**, 066801 (2012).
- ¹⁴ G. Stefanucci and S. Kurth, Phys. Rev. Lett. **107**, 216401 (2011).
- ¹⁵ P. Schmitteckert, in preparation (unpublished).
- ¹⁶ G. Stefanucci and C.-O. Almbladh, Europhysics Lett. **67**, 14 (2004).
- ¹⁷ M. Koentopp, K. Burke, and F. Evers, Phys. Rev. B **73**, 121403(R) (2006).
- ¹⁸ S. Schenk, P. Schwab, M. Dzierzawa, and U. Eckern, Phys. Rev. B **83**, 115128 (2011).
- ¹⁹ C. Verdozzi, Phys. Rev. Lett. **101**, 166401 (2008).
- ²⁰ A. Branschädel, G. Schneider, and P. Schmitteckert, Ann. Physik (Berlin) **522**, 657 (2010).
- ²¹ E. Boulat and H. M. Saleur, Phys. Rev. B **77**, 033409 (2008).
- ²² P. Schmitteckert, Phys. Rev. B **70**, R121302 (2004).
- ²³ E. Runge and E. K. U. Gross, Phys. Rev. Lett. **52**, 997 (1984).
- ²⁴ R. van Leeuwen, Phys. Rev. Lett. **82**, 3863 (1999).
- ²⁵ M. Ruggenthaler and R. van Leeuwen, EPL **95**, 13001 (2011).
- ²⁶ R. Baer, J. Chem. Phys. **128**, 044103 (2008).
- ²⁷ Y. Li and C. A. Ullrich, J. Chem. Phys. **129**, 044105 (2008).
- ²⁸ A. Branschädel, E. Boulat, H. Saleur, and P. Schmitteckert, Phys. Rev. Lett. **105**, 146805 (2010).
- ²⁹ S. T. Carr, D. A. Bagrets, and P. Schmitteckert, Phys. Rev. Lett. **107**, 206801 (2011).